# Electrohydrodynamic convection in a homeotropically aligned nematic sample

H. Richter
*Physikalisches Institut, Universität Bayreuth D-95440 Bayreuth, Germany*

A. Buka
*Research Institute for Solid State Physics, H-1525 Budapest P.O.Box 49, Hungary*

I. Rehberg
*Otto-von-Guericke-Universität, Institut für Experimentelle Physik, Postfach 4120, D-39016 Magdeburg, Germany*
(Received 25 January 1995)

Different features of electroconvection patterns at threshold in a homeotropically aligned nematic sample are studied as a function of the driving frequency and the conductivity of the sample. The primary instability is the bend Fréedericksz transition that spontaneously breaks the rotational symmetry. The director orientation is optically determined in the Fréedericksz distorted state. Stationary normal and oblique convection rolls appear as a secondary instability. A complex time dependence of the pattern at low frequencies involving a reorientation of the rolls together with the underlying director configuration is observed as predicted by theory. For low conductivity samples a transition to traveling waves is detected and the Hopf frequency is measured as a function of the driving frequency for samples with different conductivities.

PACS number(s): 61.30.Gd, 47.20.Bp

## I. INTRODUCTION

Convection in fluid layers is the most frequently used model system for the study of pattern formation [1]. Thus the thermally driven Rayleigh-Bénard convection in ordinary liquids, binary mixtures, and in liquid crystals [2], as well as electrically induced convection (EHC) in planarly aligned nematics, are to be mentioned (see [3] and references therein). The great advantage of EHC in liquid crystals compared to convection experiments in other liquids is the two easily adjustable control parameters, voltage and frequency. Additionally these systems provide different symmetries depending on the initial director alignment. In the planar configuration a preferred direction in the plane of the layer ($x$-$y$ plane) is imposed on the system.

When using homeotropic alignment with the director oriented along $z$ the basic state is rotationally symmetric in the $x$-$y$ plane. A one-dimensional model analogous to the classical Carr-Helfrich mechanism for the homeotropic alignment results in a convection pattern with wavelength considerably shorter than the sample thickness. This direct transition from the homogeneous alignment to convection is only predicted for $\epsilon_a \approx 0$ [4,5]. A lattice pattern with short wavelength was indeed observed for a $N$-($p$-methoxybenzycidene)-$p$-butylaniline (MBBA) mixture with $\epsilon_a \approx 0$ [5].

For substances with larger negative $\epsilon_a$ the rotational symmetry of the homeotropic sample is spontaneously broken by the electrically induced bend Fréedericksz transition, and convection sets in as a secondary instability. A three-dimensional linear stability analysis was carried out with the distorted director profile as an initial condition [6]. It predicts normal rolls for high driving frequencies and oblique rolls connected with a spatio-temporal chaotic state at threshold in the low frequency regime, where contrary to the planar case the velocity field exerts a torque on the director, which allows for a greater variety of patterns. This complex behavior is the motivation for the experimental investigation described in this paper.

## II. EXPERIMENTAL SETUP

The experimental setup consists of a nematic liquid crystal sandwiched between two transparent, parallel glass electrodes with spacers of 15 $\mu$m. An ac voltage is applied in the $z$ direction perpendicular to the glass plates. The nematic material MBBA with negative dielectric anisotropy is chosen for the investigation. Homeotropic alignment is achieved by coating the electrodes with lecithin. The sample temperature is controlled at $25.3 \pm 0.1\,^{\circ}$C. The measurements have been carried out with the same sample over a period of three months. During this time the conductivity has increased by about a factor of 2, resulting in a shift of the cutoff frequency of the conductive regime and enabling us to detect different scenarios.

The convection structures are observed in a polarizing microscope equipped with a 14 bit slow-scan charge-coupled device (CCD) camera with an exposure time of 0.1 s when working with only one polarizer, and an exposure time of 0.5 s, when using crossed polarizers for detection. The images are digitized with a spatial resolution of $512 \times 512$ and 16864 gray scales for each pixel.

 

## III. EXPERIMENTAL RESULTS

The first instability which occurs when increasing the field is the bend Fréedericksz transition. The experimental value of the threshold voltage of this transition was $V_F = 3.65$ V and remained constant throughout the whole observed frequency range (up to 3 kHz).

In the Fréedericksz distorted state the direction of the in plane component $\mathbf{n}_p$ of the director is arbitrary. We assume that the direction of $\mathbf{n}_p$ is constant along the $z$ direction (while its magnitude is $z$ dependent), because the homeotropic boundary conditions are not believed to support any twist. The direction of $\mathbf{n}_p$ can then be determined by rotating the sample between crossed polarizers and measuring the angle dependence of the transmitted light intensity. The spatial director variation in the $x$-$y$ plane can easily be seen by this technique. The determination of $\mathbf{n}_p$ is necessary for the characterization of the convection patterns. Rolls are defined as being normal or oblique with respect to this direction. The experimental details of the optical characterization of the patterns are presented in [7].

When the voltage is increased beyond the second threshold $V_c$, convection sets in, superposed on the Fréedericksz distorted state, leading to a roll pattern. The dependence of $V_c$ on the driving frequency [6] is shown in the phase diagram of Fig. 1. No data were taken beyond 500 Hz in order to avoid damage of the sample when applying high voltages over a long period of time.

In Fig. 2 two typical images of convection patterns are shown in an area of about 1 mm × 1 mm. In the upper part of the picture a voltage corresponding to $\varepsilon = (V^2 - V_c^2)/V_c^2 = 0.02$ at a driving frequency of 480 Hz was applied. Here the rolls are normal with respect to the orientation of $\mathbf{n}_p$. Independent contrast measurements [7] confirm this statement. The rolls are not oriented as regularly as in planarly aligned samples [10]. They are slightly bent, adjusting themselves locally to the underlying Fréedericksz direction $\mathbf{n}_p$.

Decreasing the driving frequency oblique rolls are expected according to theory [6]. In the lower part of Fig. 2 an image of the convection pattern occurring at 200 Hz and $\varepsilon = 0.02$ is presented. These rolls are oblique, as both experimental methods, namely the angular dependence of the transmitted light intensity and that of the contrast, demonstrate. Similar to the normal roll case the direction of the oblique rolls also exhibits a spatial variation in the observed area. We note that not only can the "zig" and "zag" of the two directions be seen but their superposition is also detected.

In the case of high conductivity and a cutoff frequency of about 1000 Hz, the normal rolls are stationary, while the oblique rolls show a slow time dependence similar to the one described below in Fig. 3. A further decrease of the frequency (90 Hz) leads to a much faster and thus more obvious time dependent behavior of the pattern. In Fig. 3 a time series of the rather complex pattern in

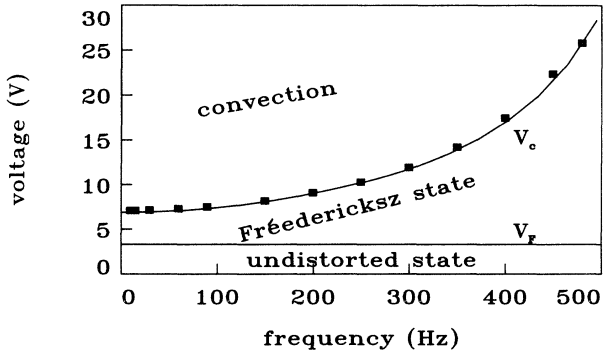


FIG. 1. Voltage-frequency phase diagram for an intermediate conductivity ($f_c = 580$ Hz).

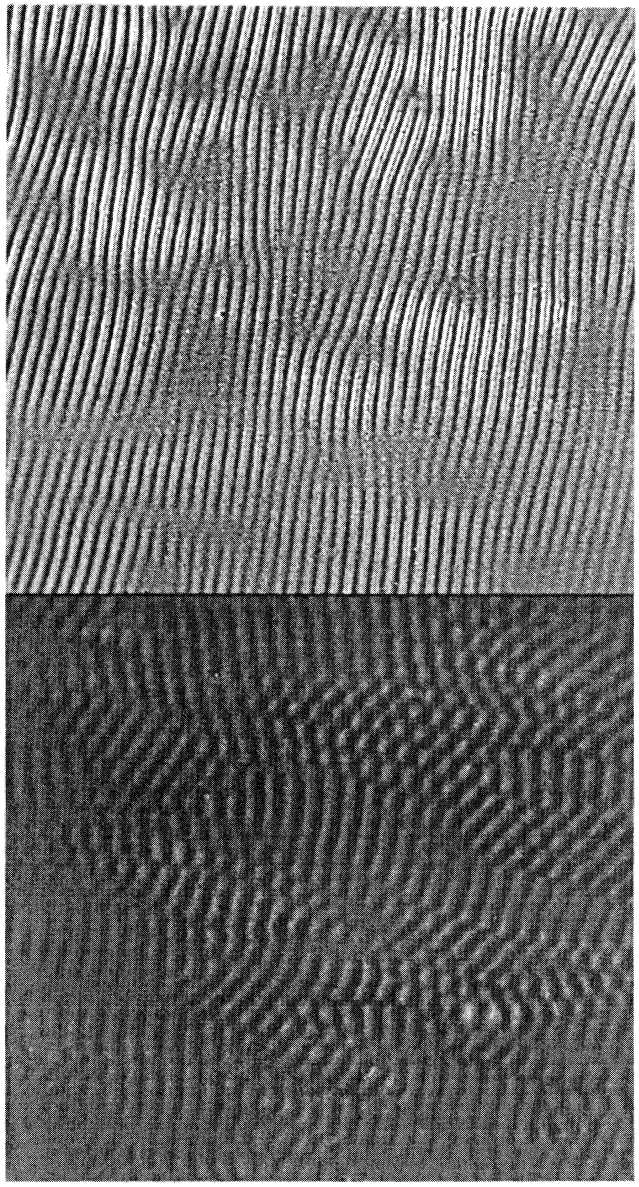

FIG. 2. Images of two typical convection patterns. Upper part: normal rolls at $f = 480$ Hz. Lower part: oblique rolls at $f = 200$ Hz ($f_c = 580$ Hz).

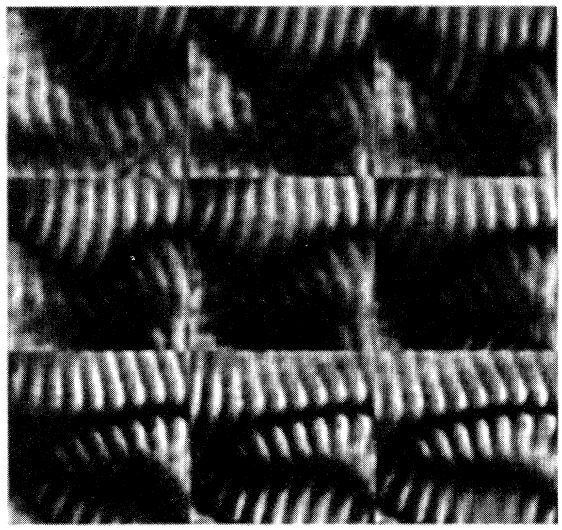

FIG. 3. Time series (by the line) of images observed between crossed polarizers at $f = 90$ Hz; time interval 20 s.

the oblique roll regime observed between crossed polarizers oriented along the edges of the pictures is shown (time interval 20 s). It can clearly be seen that not only does the convection pattern reorient, but also the director configuration changes, as indicated by the different locations of the dark and bright spots in successive pictures. For comparison, a similar time series of normal rolls at 650 Hz is given in Fig. 4. Rolls are slightly visible only in the bright parts of the pictures, where the director does not coincide with any of the polarizers' directions, contrary to the dark regions indicating total extinction [7]. The picture does not show a time dependence of the director configuration nor that of the roll direction at this frequency contrary to the measurement at 90 Hz.

For a sample with even higher conductivity ($f_c \approx$ 3 kHz) we have also observed spiral structures in the normal roll regime at some locations of the cell, see Fig. 5. Similar but more complex structures, spirals with sinusoidal traveling waves, which wind up in the center, have been seen in the dielectric regime [8].

The case of lower conductivity (cutoff frequency $f_c \approx$ 600 Hz) reveals another feature — the normal rolls travel at the onset of the instability. In the upper part of Fig. 6 a space-time series of one line over 180 s is presented, showing about an equal fraction of right and left traveling waves. In the lower part of the picture a snapshot of the convection pattern is shown. Since right traveling as well as left traveling rolls occur, it is indeed a symmetry breaking effect and not an artifact of improper adjustment of the cell.

The traveling frequency $\tilde{\omega} = v/\lambda$ of the rolls depends on the driving frequency and on the conductivity of the liquid crystal. Here $\lambda$ denotes the wavelength of the convection rolls and $v$ their velocity. The higher the driving frequency, the higher $\tilde{\omega}$ becomes, as indicated in Fig. 7. When the conductivity and thus the cutoff frequency increases, as indicated by going from curve (a) towards (c), the traveling frequency $\tilde{\omega}$ slows down until steady rolls appear at all driving frequencies.

We are aware of observations of traveling waves in planar cells [9–12] with a similar qualitative frequency dependence of the Hopf frequency $\tilde{\omega}$. Comparing the results for MBBA in planar [11,13] and in our homeotropic aligned samples, we find that the value of the Hopf frequency is of the same order of magnitude.

## IV. DISCUSSION

In summary we have shown clear evidence for the existence of oblique rolls in homeotropic alignment and the theoretically predicted spatiotemporal complexity in the oblique roll regime. This complex behavior is invoked

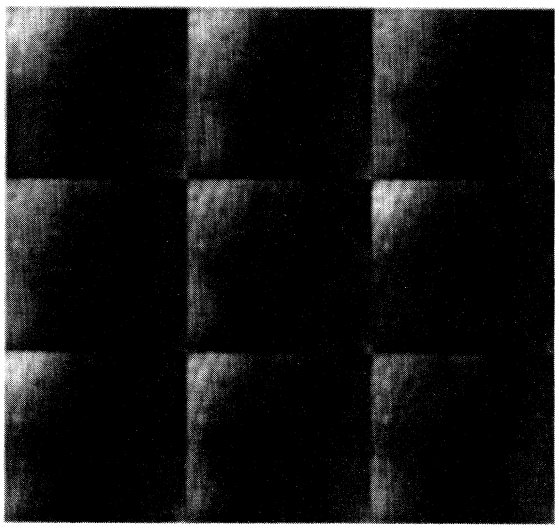

FIG. 4. Time series (by the line) of images observed between crossed polarizers at $f = 650$ Hz; time interval 20 s.

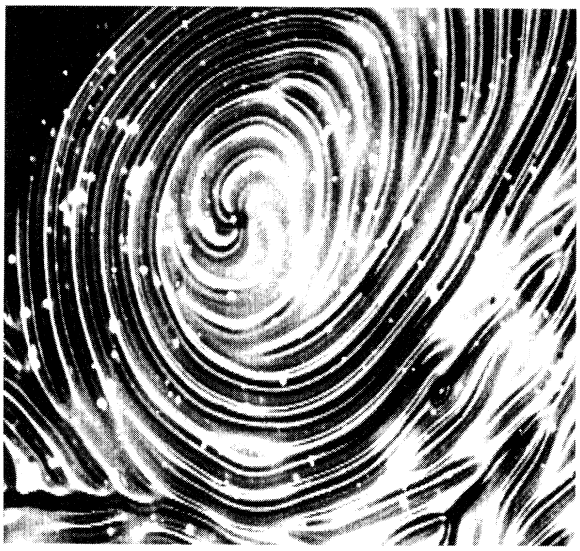

FIG. 5. Spiral structure at $f = 2.5$ kHz.

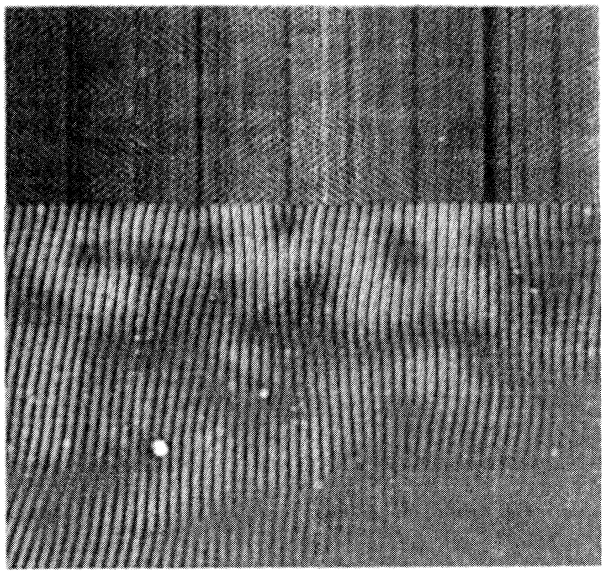

FIG. 6. Demonstration of right and left traveling rolls. Upper part: space-time series of one line over 180 s beginning from above. Lower part: snapshot of the pattern.

by the torque of the velocity field acting on the director. For small angles it is proportional to the roll angle and the square of the convection amplitude [6]. This torque vanishes for zero roll angle and thus normal rolls should be stationary. The theoretically treated, idealized situation of only one single Fréedericksz direction in the whole sample cannot be achieved experimentally because of the spontaneous symmetry breaking at the transition. Therefore a slow temporal variation of the normal rolls is also possible due to the interaction of different Fréedericksz orientations. As the experiments were performed close to threshold, results can be compared with the predictions of the amplitude equations. The theoretically calculated coherence length [14] parallel to the director is about ten times the wavelength of the rolls, which coincides with the size of regularly oriented domains in Figs. 2 and 6. The coherence length parallel to the rolls is larger than perpendicular to them as expected.

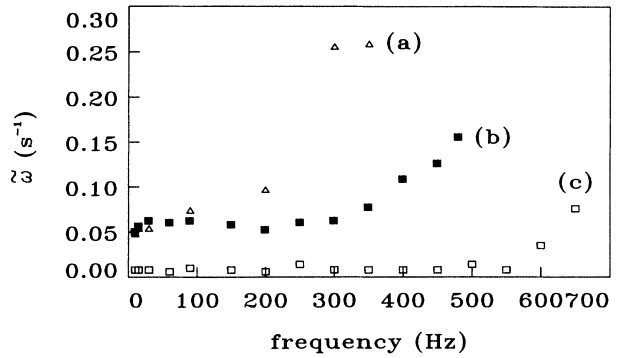


FIG. 7. Hopf frequency versus driving frequency for three different conductivities. The conductivity increases from (a) to (c). The cutoff frequencies are (a) $f_c = 450$ Hz, (b) $f_c = 580$ Hz, (c) $f_c = 850$ Hz.

The observation of traveling waves was unexpected, but is very reminiscent of similar observations in planar cells, where a successful theoretical attempt to explain a Hopf bifurcation in EHC for planar samples is in progress [15]. That theory treats the liquid crystal as a weak electrolyte with non-Ohmic conductivity, and one might expect this approach to be successful in the homeotropic case as well. Systematic investigations of $\tilde{\omega}$ for different conductivities for planar as well as homeotropic alignment are in progress in order to allow a quantitative comparison with theory. Finally the homeotropically aligned nematics provide the opportunity to study coupled amplitude equations for both the zig and zag modes and for left and right traveling waves.

## ACKNOWLEDGMENTS

We would like to thank A. Hertrich, L. Kramer, W. Pesch, and M. Treiber for stimulating discussions. The work was financially supported by Deutsche Forschungsgemeinschaft, the Volkswagen-Foundation, and by the Hungarian Academy of Sciences (OTKA 2976). H.R. received financial support from Graduiertenkolleg "Nichtlineare Spektroskopie und Dynamik," Bayreuth, and A.B. wishes to thank the University of Bayreuth for its hospitality.

[1] M. C. Cross and P. C. Hohenberg, Rev. Mod. Phys. **65**, 851 (1993).
[2] L. I. Berge, G. Ahlers, and D. S. Cannell, Phys. Rev. E **48**, R3236 (1993).
[3] L. Kramer and W. Pesch, Annu. Rev. Fluid Mech. **27**, 515 (1995).
[4] S. A. Pikin, *Structural Transformations in Liquid Crystals* (Gordon and Breach Science Publishers, New York, 1991).
[5] M. I. Barnik, L. M. Blinov, M. F. Grebenkin, S. A. Pikin, and V. G. Chigrinov, Zh. Èksp. Teor. Fiz. **69**, 1080 (1975) [Sov. Phys. JETP **42**, 550 (1976)].
[6] A. Hertrich, W. Decker, W. Pesch, and L. Kramer, J. Phys. II (France) **2**, 1915 (1992).
[7] H. Richter, A. Buka, and I. Rehberg, Mol. Cryst. Liq. Cryst. **251**, 181 (1994).
[8] S. Kai, Y. Adachi, and S. Nasuno, in *Santa Fe Institute Studies in the Sciences of Complexity*, edited by P. E. Cladis, P. Palffy-Muhoray (Addison-Wesley, 1994), New York, Vol. XXI, p. 313.
[9] K. Hirakawa and S. Kai, Mol. Cryst. Liq. Cryst. **40**, 261 (1977).

[10] I. Rehberg, B. L. Winkler, M. de la Torre Juarez, S. Rasenat, and W. Schöpf, in *Festkörperprobleme (Advances in Solid State Physics)*, edited by U. Rössler (Vieweg, Braunschweig, 1989), p. 35.
[11] A. Joets and R. Ribotta, Phys. Rev. Lett. **60**, 2164 (1988).
[12] M. Dennin, D. S. Cannell, and G. Ahlers, Mol. Cryst. Liq. Cryst. **261**, 337 (1995).
[13] I. Rehberg, S. Rasenat, and V. Steinberg, Phys. Rev. Lett. **62**, 756 (1989).
[14] E. Bodenschatz, W. Zimmermann, and L. Kramer, J. Phys. (France) **49**, 1875 (1988).
[15] M. Treiber and L. Kramer, Mol. Cryst. Liq. Cryst. **261**, 311 (1995).

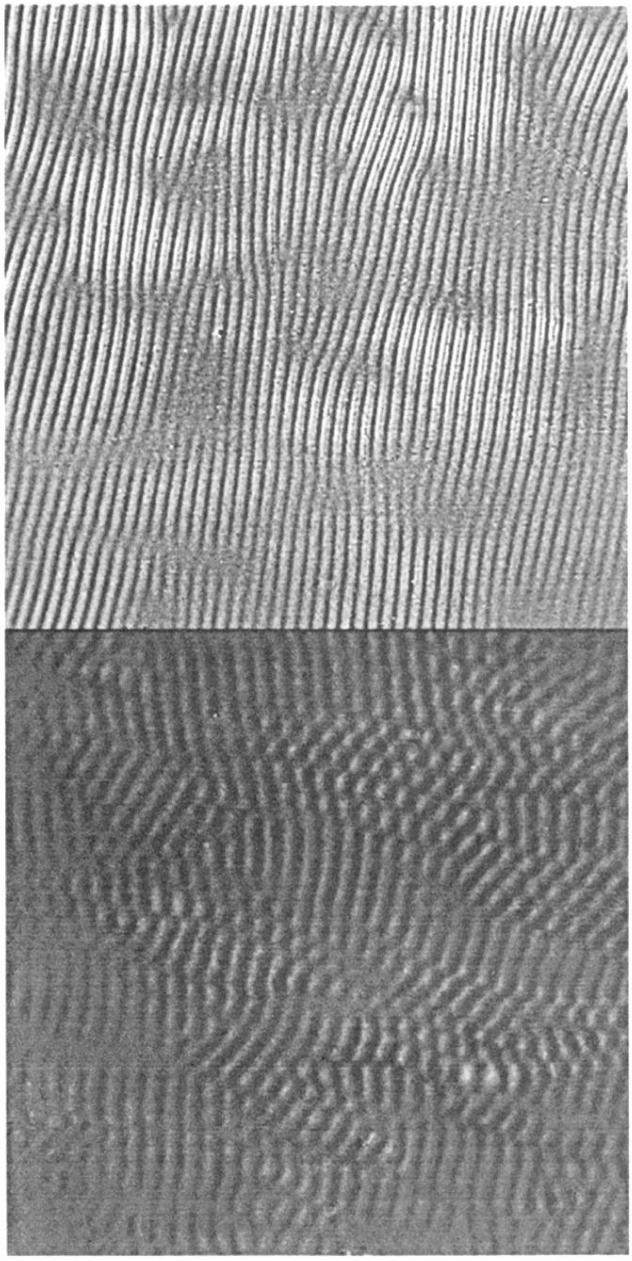

FIG. 2. Images of two typical convection patterns. Upper part: normal rolls at $f = 480$ Hz. Lower part: oblique rolls at $f = 200$ Hz ($f_c = 580$ Hz).

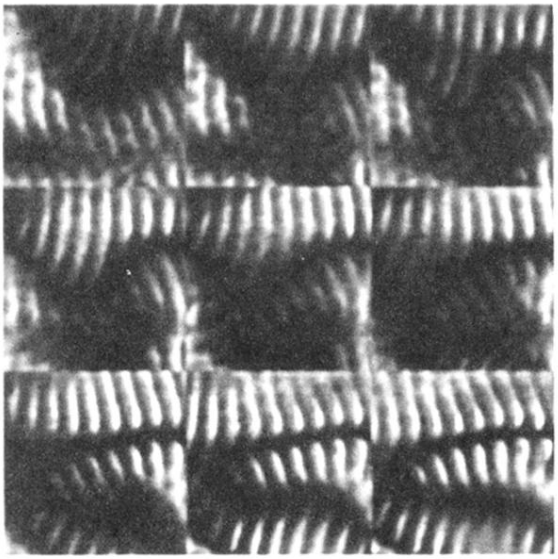

FIG. 3. Time series (by the line) of images observed between crossed polarizers at $f = 90$ Hz; time interval 20 s.

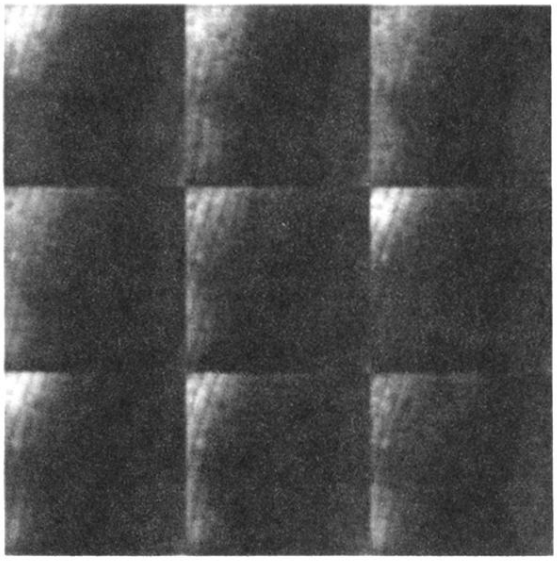

FIG. 4. Time series (by the line) of images observed between crossed polarizers at $f = 650$ Hz; time interval 20 s.

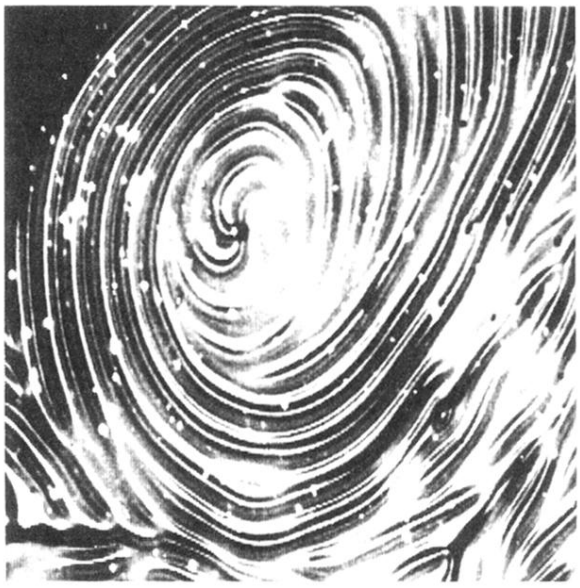

FIG. 5. Spiral structure at $f = 2.5$ kHz.

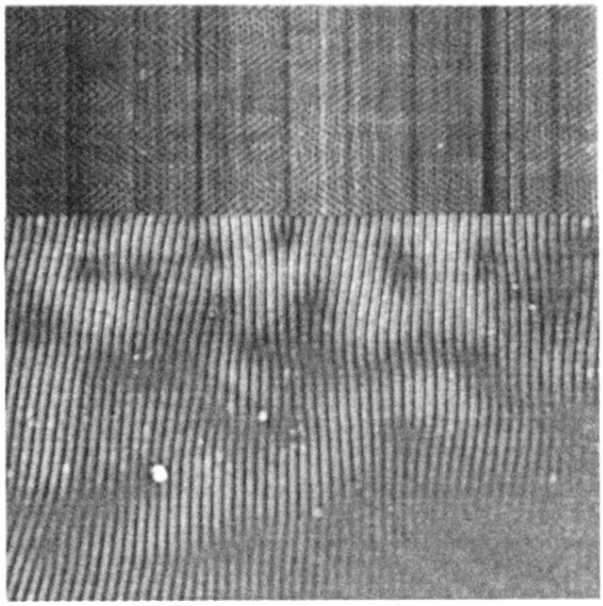

FIG. 6. Demonstration of right and left traveling rolls. Upper part: space-time series of one line over 180 s beginning from above. Lower part: snapshot of the pattern.